Journal of the European Ceramic Society 20 (2000) 775–782

Effect of nucleating agents on the crystallization behaviour and microstructure of SiO_2–CaO–MgO (Na_2O) glass-ceramics

P. Alizadeh [a,*], V.K. Marghussian [b]

[a] *Ceramic Division, Material and Energy Research Centre, Tehran, Iran*
[b] *Ceramic Division, Department of Materials Science, Iran University of Science and Technology, Narmak, Tehran, Iran*

Received 28 January 1999; received in revised form 11 April 1999; accepted 13 May 1999

Abstract

The crystallization behaviour of the ternary SiO_2–MgO–CaO system comprising different nucleating agents was investigated using DTA and XRD techniques. The effect of compositional changes on bulk crystallization and growth morphology were also studied. After a two-stage heat treatment, the phases such as wollastonite, diopside and in some cases, cristobalite, were identified. The microstructures were investigated by SEM. It was found that the pairs of $V_2O_5 + MoO_3$ and $CaF_2 + MoO_3$ are more effective nucleants compared with that of $Fe_2O_3 + WO_3$. The coarse fibrous morphology with directional surface crystallization was observed for some specimens containing $Fe_2O_3 + WO_3$ as nucleants

Keywords: Glass ceramics; Nucleating agents; Microstructure-final; Silicates; Electron microscopy (SEM)

1. Introduction

Research and development investigations pertaining to glass-ceramic materials have been underway for more than three decades.[1] The fabrication technology of glass-ceramics, the glass composition, the nature of the nucleating agent and the thermal history, all greatly affect the microstructure and properties of these materials.[2] The internal crystallization can usually be achieved with a simple two-step heat treatment. In the first step, namely the nucleation step, the mobility of atoms in the glass is sufficient for embryo formation and subsequent nuclei stabilisation. In the second step, the nuclei grow to crystals of desired sizes homogenously dispersed in the glass volume.[3] It is obvious that internal crystallization will be greatly facilitated by using suitable nucleating agents. Some investigations carried out in the field of nucleation in the ternary SiO_2–MgO–CaO and related systems have shown the relative difficulty of initiating internal nucleation and bulk crystallization in some glass-ceramic compositions of this system.[4,5]

Considering the great attention recently paid to these glass-ceramics, especially in the field of bioactive, strong glass-ceramics,[5–7] and the fact that some aspects of the nucleation and bulk crystallization in the above mentioned system are still unclear, it has been decided to conduct a comprehensive investigation on the nucleation and bulk crystallization of glasses containing SiO_2, MgO and CaO as their main constituents. In this work, the effect of several oxides on the nucleation and bulk crystallization of these glass-ceramics were investigated. The effect of compositional changes on bulk crystallization and growth morphology were also studied.

2. Experimental procedure

2.1. Melting and forming

The base glass compositions and those for the nucleating agents added to the batches are given in Table 1. All raw materials used to prepare the glasses were reagent grade. All batches were thoroughly mixed and melted in a platinum crucible in an electric furnace at 1400°C for 1 h. the melts were then quenched either in water or on a steel mould to obtain frits and bars, respectively.

* Corresponding author.

0955-2219/00/$ - see front matter
PII: S0955-2219(99)00136-3

Table 1
Chemical composition of various glasses (weight percentage)

Sample no.	SiO_2	CaO	MgO	Na_2O	Fe_2O_3	WO_3	V_2O_5	MoO_3
1	59.68	27.25	0	5.08	6	2	–	–
2	59.68	24.23	3.02	5.08	6	2	–	–
3	59.68	21.23	6.02	5.08	6	2	–	–
4	59.68	18.23	9.02	5.08	6	2	–	–
5	59.68	15.23	12.02	5.08	6	2	–	–
6	59.68	12.23	15.02	5.08	6	2	–	–
7	59.68	9.23	18.02	5.08	6	2	–	–
8	59.68	6.23	21.02	5.08	6	2	–	–
9	59.68	21.23	6.02	5.08	–	–	4	4
10	59.68	18.23	9.02	5.08	–	–	4	4
11	59.68	15.23	12.02	5.08	–	–	4	4
12	59.68	12.23	15.02	5.08	–	–	4	4
13	59.68	9.23	18.02	5.08	–	–	4	4
14	59.68	6.23	21.02	5.08	–	–	4	4

Sample no.	SiO_2	CaO	MgO	Na_2O	CaF_2	MoO_3
15	59.68	27.25	0	5.08	4	4
16	59.68	24.23	3.02	5.08	4	4
17	59.68	21.23	6.02	5.08	4	4
18	59.68	18.23	9.02	5.08	4	4
19	59.68	15.23	12.02	5.08	4	4
20	59.68	12.23	15.02	5.08	4	4
21	59.68	9.23	18.02	5.08	4	4
22	59.68	6.23	21.02	5.08	4	4

2.1.1. Heat treatment procedure

The thermal behaviour of glasses was determined using DTA technique. The DTA scans were carried out using a simultaneous thermal analyser (Polymer Laboratories, STA-1640). Ten milligrams of glassy powder sieved into fine and coarse fractions (63 and 180–212 μm) was used. The thermal analysis was made in the range 20–1100°C using powdered alumina as an inert reference material. The heating rate of 10°C/min in static atmosphere was maintained for all the DTA runs. Each glassy sample was held at its appropriate nucleation and crystallization temperatures as determined by DTA. The heating rate was 5°C/min up to the nucleation temperature and 1°C/min between the nucleation and crystallization temperatures.

For estimation of maximum nucleation rate temperature, the samples were first held for 2 h at different nucleation temperatures from T_g to $T_g + 100$°C in 20°C intervals, then, the shift of the crystallization peak to lower temperatures was measured.

2.2. Microstructural analysis

The microstructural characterization of the glass and the glass-ceramic samples were carried out by scanning electron microscope (SEM) (Cambridge, Stereoscan 360). The crystallized samples resulting from the above mentioned heat treatment schedules were then subjected to XRD using a powder diffractometer (Siemens, D-500).

3. Results and discussion

3.1. Thermal analysis

In order to evaluate the nucleation mechanisms of the glasses, samples with different specific surface areas were studied by DTA. The increase of the specific surface area does not significantly influence the glass transition temperatures, whereas for surface nucleation mechanism, the crystallization peak maxima shift relatively towards lower temperatures.[3] The exothermic crystallization peak temperatures for glasses with various nucleating agents and two particle size ranges are given in Table 2. ΔT values in Table 2 are the difference between peak temperatures for two particle size ranges.

Some of the glass samples mentioned in Table 2 showed relatively small difference in DTA peak positions and were anticipated to undergo bulk nucleation. These low ΔT values can be attributed to various thermodynamic and kinetic factors. Fig. 1 shows the exothermic crystallization

Table 2
Crystallization peak temperatures of two particle sizes for various samples

Sample no.	% MgO	Particle size (μm)	T_p (°C)	ΔT
1	0	< 63	895	36
		180–212	931	
2	3.02	< 63	904	41
		180–212	945	
3	6.02	< 63	895	27
		180–212	922	
4	9.02	< 63	872	55
		180–212	927	
5	12.02	< 63	876	41
		180–212	917	
6	15.02	< 63	867	52
		180–212	919	
7	18.02	< 63	871	40
		180–212	911	
8	21.02	< 63	873	40
		180–212	913	
9	6.02	< 63	859	26
		180–212	885	
10	9.02	< 63	837	22
		180–212	859	
11	12.02	< 63	834	34
		180–212	868	
12	15.02	< 63	838	26
		180–212	864	
13	18.02	< 63	837	25
		180–212	862	
14	21.02	< 63	837	26
		180–212	863	
15	0	< 63	860	22
		180–212	882	
16	3.02	< 63	827	17
		180–212	844	
17	6.02	< 63	866	23
		180–212	889	
18	9.02	< 63	856	23
		180–212	879	
19	12.02	< 63	850	33
		180–212	888	
20	15.02	< 63	864	31
		180–212	895	
21	18.02	< 63	856	24
		180–212	880	
22	21.02	< 63	865	30
		180–212	895	

peaks for three samples of similar composition but containing different nucleants. The sample no. 20 with $\Delta T = 31°C$ reveals the highest intensity in crystallization peak, whereas the sample no. 12 with a lower ΔT value has a medium crystallization peak intensity. It is obvious that a low ΔT value while rightly indicating the possibility of bulk nucleation occurrence, is not directly related to the kinetics of growth process.

It has been reported that the presence of flourides, e.g. CaF_2, greatly enhance the crystallizability of some glasses.[8] As a result of viscosity decrease, brought about by the addition of flourides, the mobility of different ions and ionic complexes during the crystallization process of glasses will be markedly increased, leading to higher crystallizabilities.[9] In this way the effective bulk nucleation and especially relatively fast crystal growth in flouride containing samples, e.g. sample no. 20, can be explained by kinetic factors.

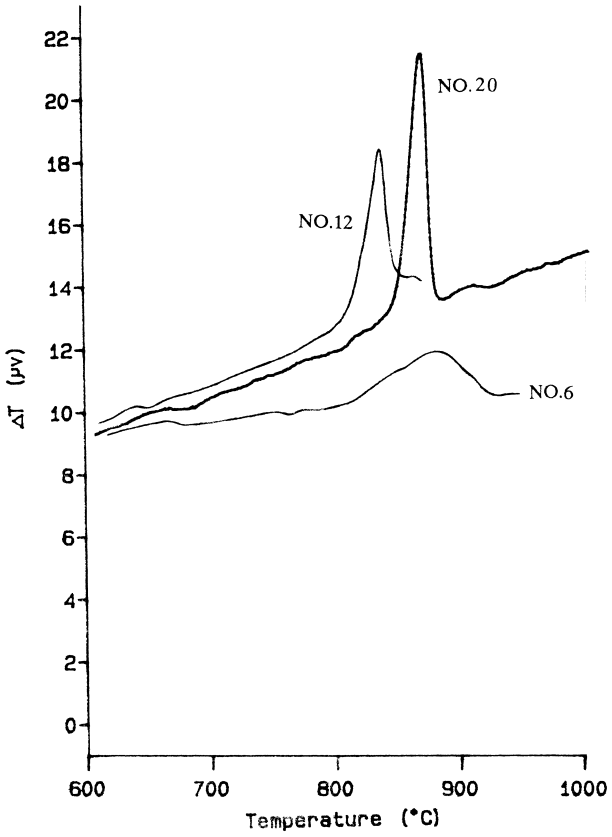

Fig. 1. DTA curves for sample nos. 6, 12 and 20 with particle size < 63 μm.

On the other hand, the lowest crystallization peak temperatures along with generally low ΔT values were found in samples containing V_2O_5 and MoO_3 nucleating agents (sample nos. 9–14), indicating the occurrence of effective bulk nucleation in them. It is known that V_2O_5 greatly reduces the surface tension of glasses,[10] therefore, it seems that the presence of this oxide in glass sample nos. 9–14, resulted in lower crystal-liquid interfacial energies and lower thermodynamic free energy barriers for nucleation. The relatively lower crystallization peak intensity in sample no. 12, as an example of this group, [as compared with sample no. 20 (Fig. 1)], can probably be attributed to lower growth kinetics.

Sample no. 6 containing $Fe_2O_3 + WO_3$ nucleants having the highest ΔT value showed the lowest intensity in crystallization peak (Fig. 1). Therefore, it can be concluded that the occurrence of an effective bulk nucleation leading to volume crystallization is impossible in this case and surface crystallization is the dominant mechanism.

Fig. 2 shows the variation of $(T_p - T'_p)$ versus heat treatment temperatures for sample no. 3, where T_p and T'_p are the crystallization peak temperatures of the as-quenched and previously nucleated samples, respectively. The maximum in this curve, which is similar to nucleation versus temperature curves, indicates the optimum nucleation temperature.[11] In this way, the nucleation and crystallization temperatures for bulk samples were determined as 700 and 980–1000°C, respectively, for sample nos. 1–8, 680 and 910–930°C for sample nos. 9–14 and 675 and 930–960°C for sample nos. 15–22.

3.2. XRD analysis

The XRD patterns for sample nos. 1–8 are shown in Fig. 3. The only phase detected by X-ray in sample no. 1 was wollastonite. However, diopside was also detected in other patterns. Cristobalite in minor amounts is also present. On the basis of Fig. 3, it can be stated that by increasing the content of MgO at the expense of CaO, the peak intensity of wollastonite decreases while the peak intensity of diopside phase increases, as expected.

The XRD patterns for sample nos. 9–14 are shown in Fig. 4. In this group of samples the intensity of cristobalite phase appears to be higher in comparison with other groups, and in sample no. 14 a magnesium silicate phase (JCPDS 11-273) is clearly observed.

The XRD patterns for sample nos. 15–21 are shown in Fig. 5. It is observed that the peak intensities of wollastonite and diopside in these samples are higher than the sample nos. 1–8 and 9–14. (This is in agreement with DTA curves.) Along with diopside and wollastonite, cristobalite is also present in these samples. Table 3 summerizes the existing phases in various samples, which are wollastonite, diopside, cristobalite and magnesium silicate.

It can be concluded that, in addition to bulk composition, the nucleating agent influences the nature and amount of the phases developed after heat treatment. For example, with comparison of Figs. 3–5, it is

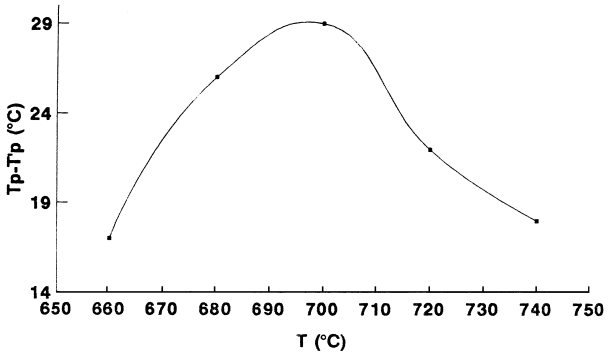

Fig. 2. $T_p - T'_p$ difference versus heat treatment temperature for sample no. 3.

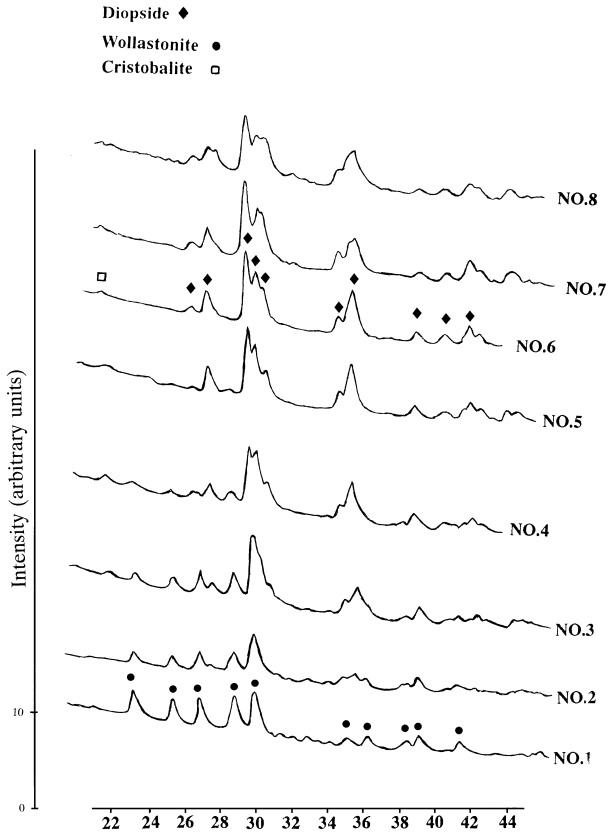

Fig. 3. XRD patterns of sample nos. 1–8.

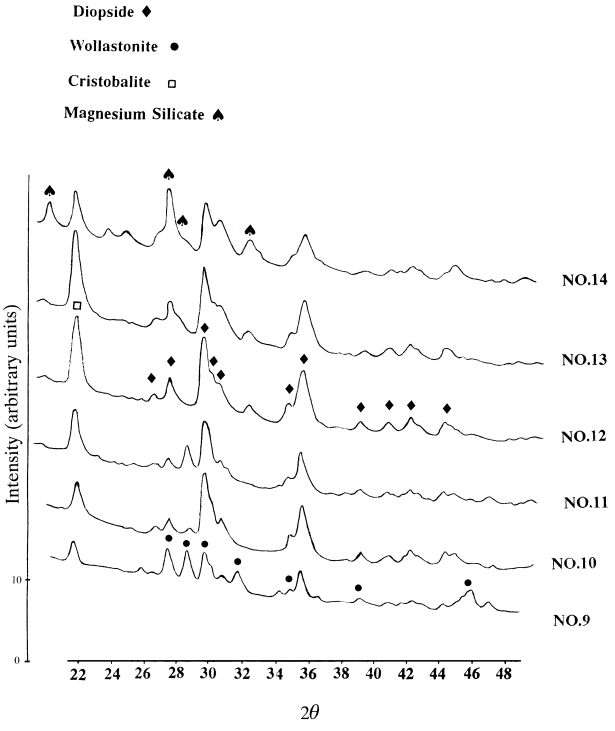

Fig. 4. XRD patterns of sample nos. 9–14.

concluded that the presence of a mixture of V_2O_5 and MoO_3 as nucleating agents promoted the formation of cristobalite, while with Fe_2O_3 and WO_3 the formation of this phase is retarded. In order to discover the exact reasons behind this observation, further work is required. Also with the former nucleating agents, the formation of magnesium silicate facilitated in comparison with other nucleants.

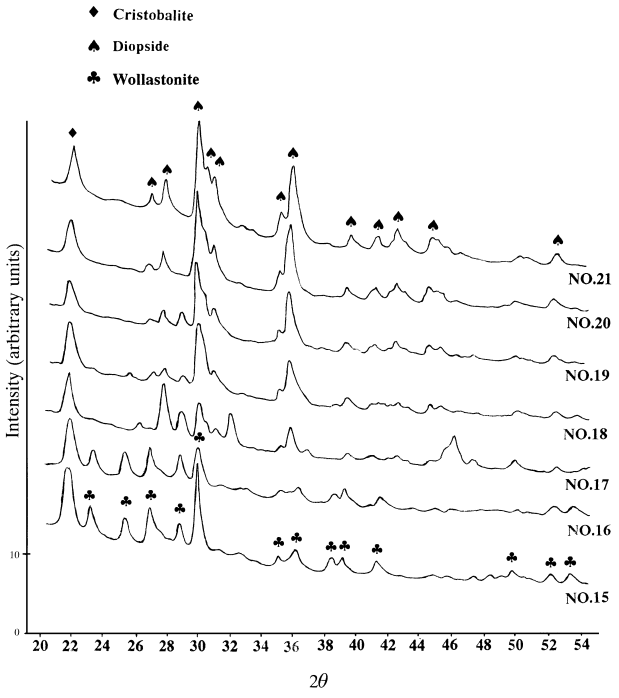

Fig. 5. XRD patterns of sample nos. 15–21.

Table 3
X-ray diffraction results for the heat treated glass-ceramics

Sample no.	Crystalline phases
1	Wollastonite
2	Wollastonite–diopside
3	Wollastonite–diopside–cristobalite[a]
4	Wollastonite–diopside–cristobalite[a]
5	Diopside–wollastonite[a]–cristobalite[a]
6	Diopside–cristobalite[a]
7	Diopside–cristobalite[a]–magnesium silicate[a]
8	Diopside–cristobalite[a]–magnesium silicate[a]
9	Wollastonite–diopside–cristobalite
10	Wollastonite–diopside–cristobalite
11	Wollastonite–diopside–cristobalite
12	Diopside–cristobalite
13	Diopside–cristobalite–magnesium silicate[a]
14	Diopside–cristobalite–magnesium silicate
15	Wollastonite–cristobalite
16	Wollastonite–cristobalite
17	Wollastonite–diopside–cristobalite
18	Diopside–wollastonite[a]–cristobalite
19	Diopside–wollastonite[a]–cristobalite
20	Diopside–cristobalite
21	Diopside–cristobalite

[a] Phases present in minor amounts.

3.3. Microstructural characterization

It is of interest to compare the microstructures of sample nos. 3, 9 and 17 with the same composition and different nucleants with each other (Figs. 6–8). EDAX analyses taken from sample nos. 3 and 9 showed that both contained wollastonite particles along with fibrous crystals of diopside which in the case of sample no. 9 are much finer. The EDAX analysis of sample no. 3, shown in Fig. 9, reveals the existence of iron peak in the diopside EDAX analysis indicating the replacement of Mg^{2+} by Fe^{+2} or Fe^{+3} as reported by other researchers.[12] On the other hand, it seems that the very efficient

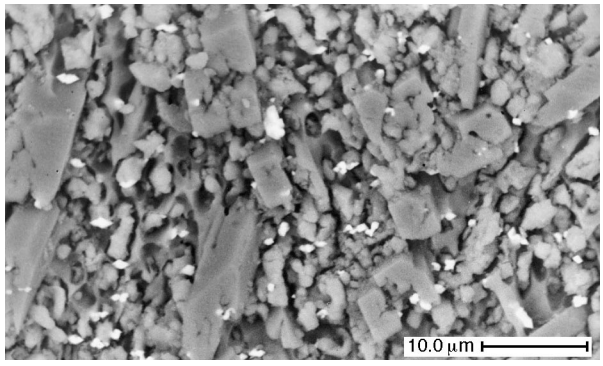

Fig. 6. SEM micrograph of glass-ceramic no. 3.

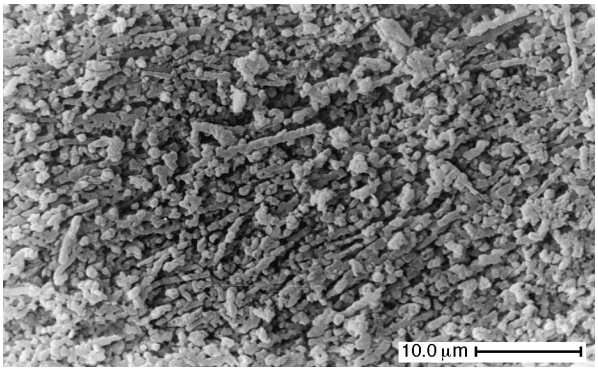

Fig. 7. SEM micrograph of glass-ceramic no. 9.

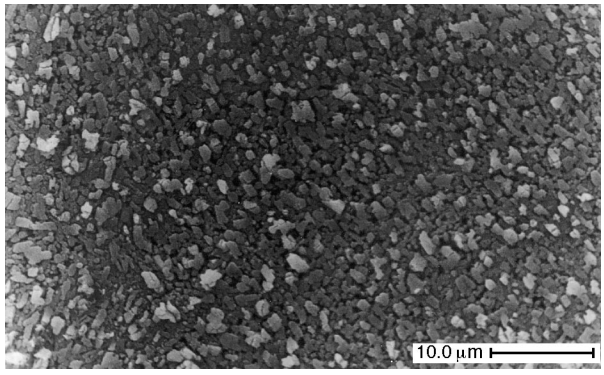

Fig. 8. SEM micrograph of glass-ceramic no. 17.

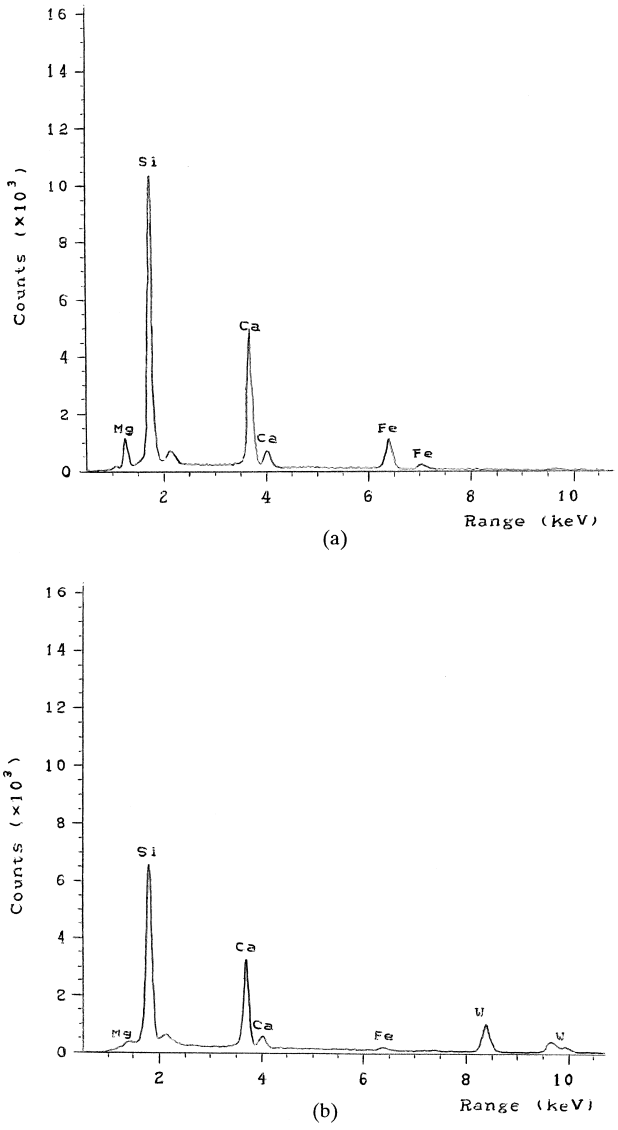

Fig. 9. The EDAX analysis of sample no. 3; (a) diopside; (b) wollastonite.

nucleation achieved in sample no. 17 by addition of CaF_2 and MoO_3 caused the crystals to impinge on each other before they have grown much more than 1 μm, resulting in a fine microstructure.

The comparison of sample nos. 6, 12 and 20 (with the same composition and different nucleants), also showed, (Figs. 10–12), that while sample no. 12 containing $V_2O_5 + MoO_3$ as nucleants exhibited a very fine microstructure containing miniature fibres, sample no. 6 with the same composition and different nucleants, ($Fe_2O_3 + WO_3$), showed coarse fibrous morphology with directional surface crystallization. This can again be attributed to a $V_2O_5 + MoO_3$ nucleant combination being more effective than that of $Fe_2O_3 + WO_3$. The relative ineffectiveness of the nucleants in sample no. 6 which is apparent from the DTA results in Table 2, has led to surface crystallization. Fig. 13 shows the morphology

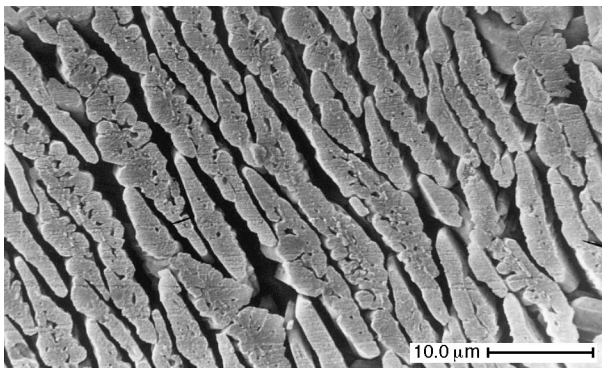

Fig. 10. SEM micrograph of glass-ceramic no. 6.

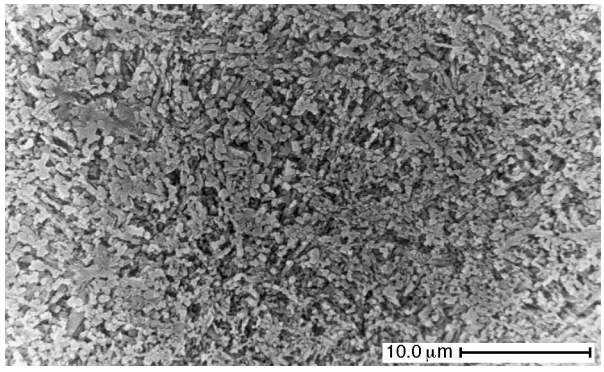

Fig. 11. SEM micrograph of glass-ceramic no. 12.

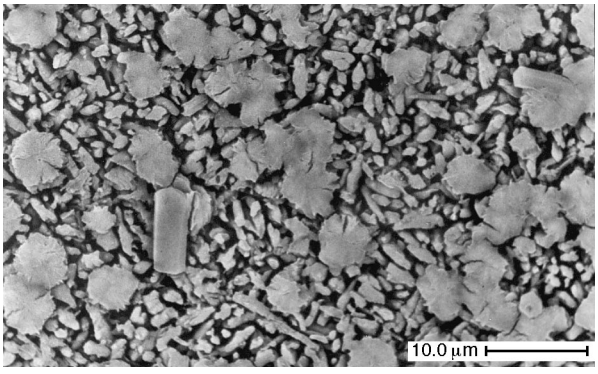

Fig. 12. SEM micrograph of glass-ceramic no. 20.

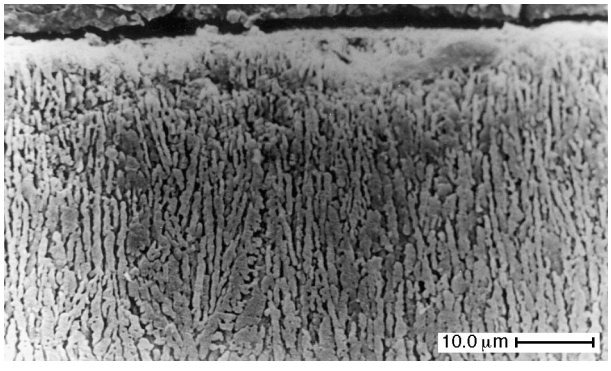

Fig. 13. Surface crystallization in sample no. 6.

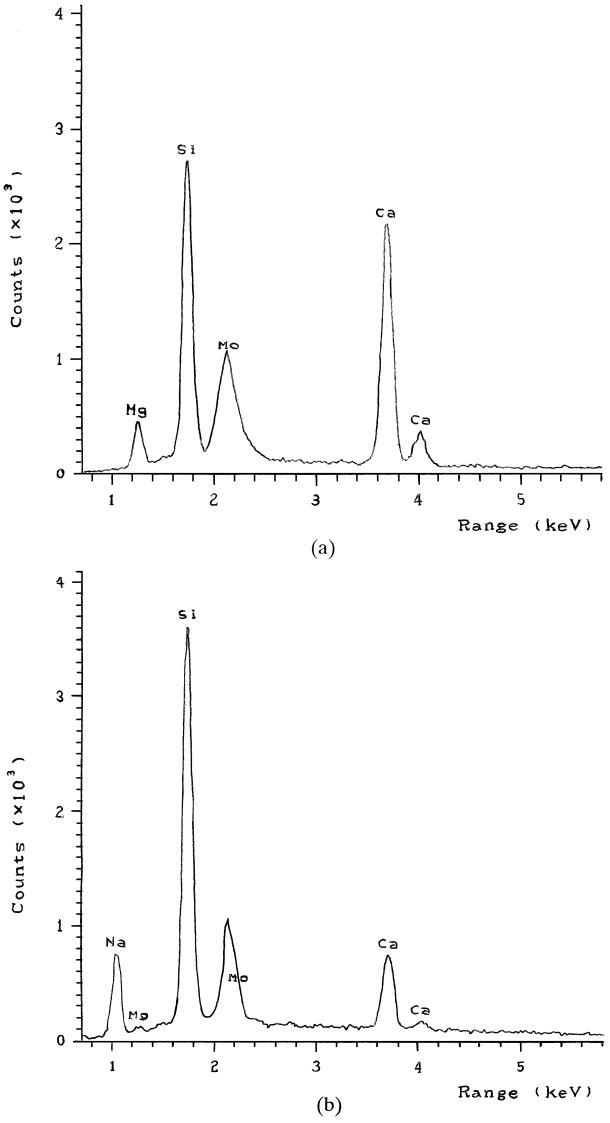

Fig. 14. The EDAX analysis of sample no. 20; (a) diopside; (b) sodium silicate.

of fibrous diopside phase which grew perpendicularly to the surface.

Sample no. 20 (Fig. 12) with $CaF_2 + MoO_3$ nucleants, gave smaller diopside crystals (as proved by EDAX) with less developed fibrous morphology, owing to the same effective nucleation mechanism discussed above. The EDAX analysis of sample no. 20 (Fig. 14) shows that the main crystalline phase appeared as fine crystals is diopside. The presence of other silicate phases were also detected by EDAX in sample no. 20. These well grown phases, which were sodium and calcium silicates exhibiting cylindrical and spherulitic morphologies, respectively, were not detectable by XRD patterns.

The microstructure of sample no. 15 is shown in Fig. 15. This sample is a typical example of samples containing CaF_2 and MoO_3 nucleants exhibiting a fine

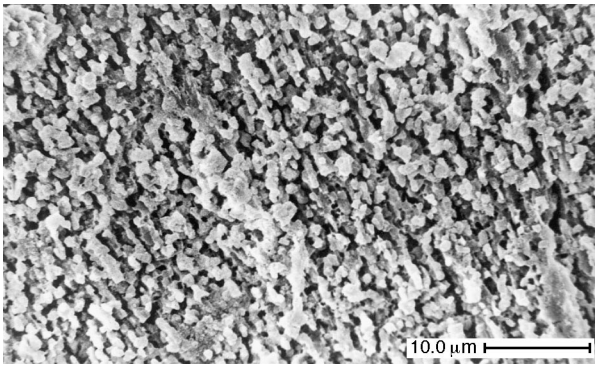

Fig 15. SEM micrograph of glass-ceramic no. 15.

microstructure containing wollastonite and cristobalite as the major and minor phases, respectively.

The fine microstructures developed in the presence of CaF_2 and MoO_3 nucleants as well as the greatly enhanced crystallizability of the samples containing these nucleants (as stated previously) can be attributed to the structural changes as follows:

A general effect of the introduction of flourine would be to replace strong Si–O–Si linkages by pairs of Si–F linkages with the result of weakening effect on the glass network. [8] This can affect the nucleation and especially growth kinetics.

After heat treatment, millimeter sized pores were observed in sample nos. 18–20. Density measurements showed that the densities of glass-ceramics were much higher than the parent glass in these samples (for example, the densities of glassy sample no. 20 and its glass-ceramic counterpart were found to be 2.63 and 3.35 g/cm^3, respectively). The densities of diopside and wollastonite are 3.39 and 2.8 g/cm^3, respectively. Therefore it is expected that the samples containing diopside as the major crystalline phase in great amounts (all these samples showed high crystallinity) are generally more susceptible to pore formation owing to the density differences between crystalline phases and glassy residue.

4. Conclusions

1. With attention to difference in crystallization peak temperatures due to different particle sizes (ΔT parameter) and microstructural investigations, it can be concluded that if $\Delta T < 40°C$ the occurrence of a certain degree of bulk nucleation can be expected (in some cases along with surface crystallization) in the glass samples, whereas for specimens with $\Delta T > 40°C$ mainly surface crystallization can be observed. Therefore, for the compositions investigated in this work $V_2O_5 + MoO_3$ and $CaF_2 + MoO_3$ pairs had the ability of inducing bulk nucleation, whereas $WO_3 + Fe_2O_3$ pair (with some exceptions) were relatively ineffective in this respect.

2. In addition to the ΔT parameter, the sharpness of crystallization peak and the peak temperature are other factors showing the occurrence of bulk nucleation and the susceptibility of samples to volume crystallization. In this respect it was shown that $CaF_2 + MoO_3$ pair greatly enhances the crystallinity of these glass ceramics.
3. In the present investigation, the mixture of Fe_2O_3 and WO_3 retards the formation of cristobalite after heat treatment, while the mixture of V_2O_5 and MoO_3 intensifies the formation of this phase.
4. In the present investigation, glass-ceramics containing $Fe_2O_3 + WO_3$ and $V_2O_5 + MoO_3$ nucleants, a dendritic morphology was observed whereas in the glass-ceramics containing $CaF_2 + MoO_3$, a very fine microstructure composed of equiaxed grains was developed.

References

1. Övecoglu, M. L., Kuban, B. and Özer, H., Characterization and crystallization kinetics of a diopside-based glass-ceramic developed from glass industry raw materials. *J. Eur. Ceram. Soc.*, 1997, **17**, 957–962.
2. Chu, J. I., Park, H. C. and Sorrell, C. C., DTA study of nucleation and crystallization of $MgO–CaO–SiO_2–P_2O_5$ glass-ceramics containing ZrO_2, $BaCO_3$ and Li_2CO_3. *Int. Ceram. Monogr.*, 1994, **1**, 585–590.
3. Leonelli, C., Manfredini, T. and Paganelli, M., Crystallization of some anorthite-diopside glass precursors. *J. Mat. Sci.*, 1991, **26**, 5041–5046.
4. Baldi, G., Generali, E. and Leonelli, C., Effects of nucleating agents on diopside crystallization in new glass-ceramics for tile-glaze application. *J. Mat. Sci.*, 1995, **30**, 3251–3255.
5. Kokubo, T., Ito, S., Sakka, S. and Yamamuro, T., Formation of a high-strength bioactive glass-ceramic in the system $MgO–CaO–SiO_2–P_2O_5$. *J. Mat. Sci.*, 1986, **21**, 536–540.
6. Liu, D. M. and Chou, H. M., Formation of a new bioactive glass-ceramic. *J. Mat. Sci., Mat. Med.*, 1994, **5**, 7–10.
7. Kokubo, T., Ito, S., Hayashi, T., Sakka, S., Kitsugi, T., Yamamuro, T., Takagi, M. and Shibuya, T., Structure and properties of a load-bearable bioactive glass-ceramic. Collected papers, XIV Intl. Congr. on Glass, 1986, pp. 408–415.
8. Omar, A. A., El-Shennawi, A. W. A. and Khater, G. A., The role of Cr_2O_3, LiF and their mixtures on crystalline phase formation and microstructure in Ba, Ca, Mg aluminosilicate glass.. *Br. Ceram. Trans. J.*, 1991, **90**, 179–183.
9. Hill, R. and Wood, D., Apatite-mullite glass-ceramics. *J. Mat. Sci., Mat. Med.*, 1995, **6**, 311–318.
10. Hlavac, J., *The Technology of Glass and Ceramics*. Elsevier Science Publishing Company, New York, 1983 (p. 80).
11. Bryden, R. H. and Caley, W. F., Determination of nucleation temperature of a lime aluminosilicate glass-ceramic by differential thermal analysis. *J. Mat. Sci. Lett.*, 1997, **16**, 56–58.
12. Putnis, A., *Introduction to Mineral Sciences*. Cambridge University Press, Cambridge, 1992 (p. 152).